Hindawi Publishing Corporation
Advances in Materials Science and Engineering
Volume 2013, Article ID 838943, 9 pages
http://dx.doi.org/10.1155/2013/838943

Research Article

Damage Simulation and Ultrasonic Detection of Asphalt Mixture under the Coupling Effects of Water-Temperature-Radiation

Yong-chun Cheng, Peng Zhang, Yu-bo Jiao, Ye-dan Wang, and Jing-lin Tao

College of Transportation, Jilin University, Changchun 130025, China

Correspondence should be addressed to Yu-bo Jiao; jiaoyubo86@163.com

Received 26 May 2013; Accepted 8 October 2013

Academic Editor: Aiguo Xu

In order to accurately simulate the performance changes of asphalt pavement in the hot rainy days, laboratory water-temperature-radiation cycle test is designed and carried out for the damage simulation of asphalt mixture under the environmental effect of rain, high temperatures, and sunshine. Ultrasonic detection method is used to determine the ultrasonic velocity of asphalt mixture specimen under different temperatures and water contents in the process of water-temperature-radiation cycles. Thus, we get the preliminary damage assessment. Splitting strength attenuation is defined as the damage parameter. In addition, the regression prediction models of the ultrasonic velocity and damage coefficient of asphalt mixture are constructed using the grey theory, neural network method, and support vector machine theory, respectively. We compare the prediction results of the three different models. It can be concluded that the model derived from the support vector machine possesses higher accuracy and stability, which can more satisfactorily reflect the relationship between ultrasonic velocity and damage coefficient. Therefore, the damage degree of the asphalt mixture can be obtained.

1. Introduction

The strength of asphalt mixture is critical to the performance of asphalt pavement in the hot rainy days in summer [1, 2]. Under the combined effects of the external factors, such as the frequent alternated changes of rain, high temperatures as well as sunshine, and the traffic load, serious premature damage of asphalt pavement will appear. The premature damage not only affects the road performance, but also increases the cost of road maintenance. At present, studies have been done on the effect of only single or dual factors of rain, temperature, and sunshine on asphalt mixture. Tan et al. [3] made a series of tests on low temperature performance of asphalt mixture under the action of moving water and found that moving water had more effect on the asphalt mixture with larger porosity and asphalt viscosity; Li and Tong [4] studied the aging effects of the asphalt mixture under the action of ultraviolet rays in the desert regions. The results showed that the impact of ultraviolet aging manifested longer time than that of thermal aging for asphalt. Jiang et al. [5] studied the performance changes of asphalt mixture under the dual effects of 60°C and hydrodynamic erosion; the results revealed that the viscosity of asphalt mastic reduced and aggregate adhesion decreased as well, resulting in the failure by shear. As can be seen from the current research status, the effects of rain, temperature, and sunshine on asphalt mixture are considered just from single or dual factors. Therefore, it is very necessary to study the performance attenuation law of asphalt mixture under the combined action of water, temperature and sunshine for its durability design.

At present, the ultrasonic nondestructive testing method has been widely used in the field of civil engineering, especially in the concrete detection. In addition, ultrasonic testing technology has been involved in test specification by certain countries [6]. However, performance evaluation method of asphalt mixture is still based on specimen destructive testing, and the application of ultrasonic in the damage identification for asphalt mixture is just at the initial stage. Tigdemir et al. [7] successfully estimated the fatigue life of asphalt mixture by using the changes of ultrasonic velocity. Yi et al. [8] introduced ultrasonic test method to the freeze-thaw test of the asphalt mixture, and ultrasonic velocity

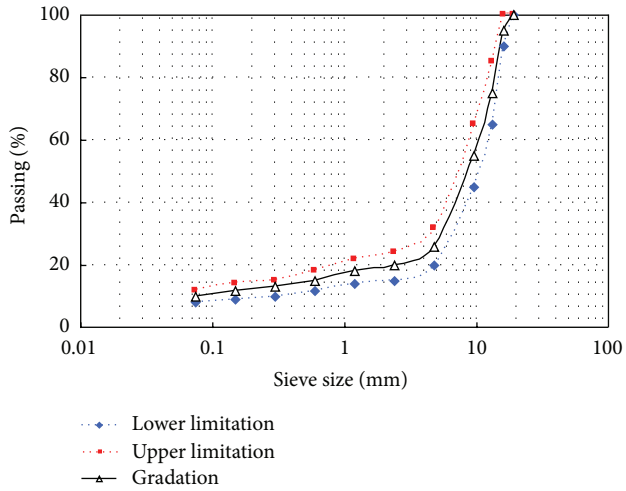

Figure 1: Grading curve of SMA-16.

was applied to characterize its freeze-thaw splitting strength. These researches establish the mathematical relationship between velocity and testing indicators based on the least squares method, so as to obtain the appropriate mechanical indicators. However, the least squares regression modeling method is simple, low precise, and cannot analyze the random effect variables. Although this method may have a good effect in some particular regions, its generalization ability is unsatisfactory [9].

In this paper, the water-temperature-radiation (W-T-R) cycle test in the laboratory is introduced to simulate the damage of asphalt pavement under the effect of rainfall, high temperature and sunshine in summer. The damage degree in internal structure of asphalt mixture is achieved by comparing the changes of ultrasonic parameters. The methods of grey theory, neural network, and support vector machine are used to establish the damage regression models for prediction of asphalt mixture under the action of W-T-R cycles. The results reveal that the ultrasonic detection method based on support vector machine can more quickly and effectively evaluate the damage state of asphalt mixture under the actions of W-T-R cycles.

2. Experimental Procedures and Modeling Principles

2.1. Experimental Procedures

2.1.1. W-T-R Cycle Test. The asphalt tested is Pan Jin-AH90# heavy traffic asphalt. The asphalt parameters, such as penetration, softening point, ductility, flash point, and density, are tested in accordance with the specified method, as listed in Table 1. Test gradation is SMA-16, which is often used for highway upper layer. Grading curve is shown in Figure 1. In order to control the asphalt film thickness and porosity, the specimens are divided into five groups, that is, A, B, C, D, and E, according to different asphalt-aggregate ratio and striking times; the molding process of each group is shown in Table 2.

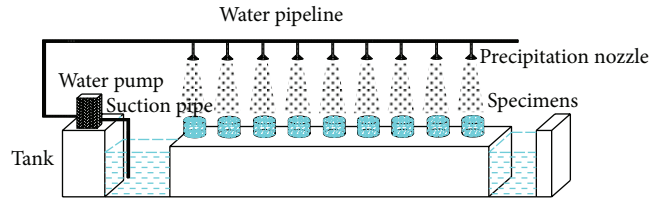

Figure 2: Rainfall simulation system.

The rainfall simulation system is installed in constant temperature room at 20°C for simulating hydrodynamic erosion to pavement, as shown in Figure 2. This system is made up of water pump, tank, pipeline, and precipitation nozzle. It can simulate rainfall with 30 mm/d, which is equal to the heavy rainfall (25 mm/d~50 mm/d).

The ultraviolet lamp tubes are installed in the insulation box under 60°C for simulating the action of high temperature as well as sunshine to asphalt pavement. There are totally 6 ultraviolet lamps, and the power of each ultraviolet lamp is 20 W. The surface area of heat preservation box is about 6 m^2. Thus, the radiant quantity can reach 2000 mW/m^2, which is 5.3 times more than the maximum radiant amount of natural light. In this case, this system can effectively simulate the radiant interactions of strong sunshine.

The treatment of W-T-R cycle test is as follows. First, the specimen is washed by simulant rainfall for 12 h at 20°C (as shown in Figure 3(a)). Then, it is put in 60°C incubator with high radiation for 12 h (as shown in Figure 3(b)). Each specimen is subjected to 12 cycles.

2.1.2. Ultrasonic Detection of Asphalt Mixture. Nonmetallic ultrasonic monitor (ZBL-U520/510, Beijing ZBL Science & Technology Co., Ltd., China) is used for the detection of asphalt mixture specimen. In order to reduce the acoustic energy loss, vaseline is smeared on the contact surface of specimen and the probe as couplant. Considering the nonuniformity of the asphalt mixture, five ultrasonic measuring points are uniformly arranged on each specimen, as shown in Figure 4.

2.2. Modeling Principles

2.2.1. Support Vector Machine Theory. Support Vector Machine (SVM) is a new learning theory built on VC dimension theory and structural risk minimization principle [10–12]. SVM has many unique advantages in solving the problems of small samples, nonlinear, and high-dimensional pattern recognition. Its result is a global optimal solution with strong generalization ability [13]. The basic idea of SVM theory focuses on defining the optimal linear hyperplane, and the algorithm of finding the optimal linear hyperplane is attributed to the solution of a convex programming problem. And then, based on Mercer expansion theorem, the sample space is mapping into a high dimensional feature space (Hilbert space) by using nonlinear mapping. Therefore, the method of linear learning machine in the feature space can

Table 1: The technical parameters of tested asphalt.

Technical parameters	25°C penetration (0.1 mm)	Softening point (°C)	15°C ductility (cm)	Penetration index	15°C density (g/cm^3)
Test Results	86	46	189.2	−1.461	1.081
Technical requirements	80~100	>44	>130	−2~2	Measured

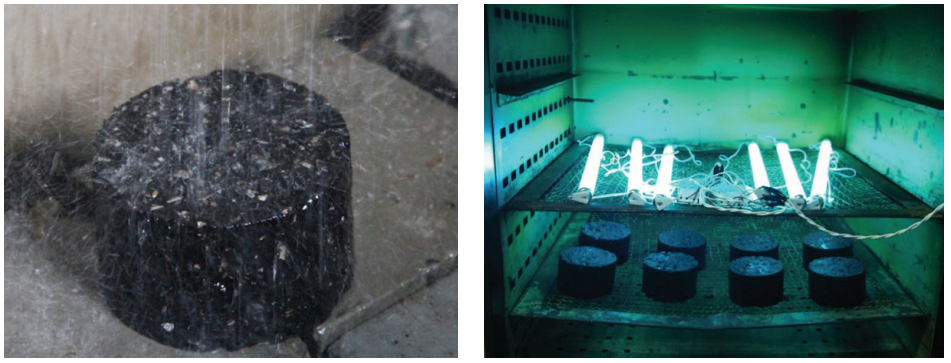

(a) Hydrodynamic erosion test (b) High temperature radiation test

Figure 3: Pretreatment method on specimen.

Table 2: Modeling process of specimen.

Specimen group	Striking times	Asphalt-aggregate ratio
A	Double-sided strike 75 times	3.5%
B	Double-sided strike 75 times	3.0%
C	Double-sided strike 75 times	4.5%
D	Double-sided strike 50 times	3.5%
E	Double-sided strike 90 times	3.5%

be used to solve the problems of high nonlinear classification and regression in sample space [14, 15].

For the linear regression problems, the data samples are n-dimensional vector, and the l-sample set in given area is

$$(x_1, y_1), \ldots, (x_l, y_l) \in R^n \times R, \tag{1}$$

where x_i is input variable; y_i is output value.

Linear regression function is as follows:

$$f(x) = \omega \cdot x + b, \tag{2}$$

where $\omega \cdot x$ is innerproduct; $b \in R$ is threshold value.

The weight vector ω can be obtained by introducing Lagrange' multipliers and the use of duality principle for optimization:

$$\omega = \sum_{i=1}^{l} (\alpha_i - \alpha_i^*) x_i, \tag{3}$$

where α_i, α_i^* are Lagrange' multipliers.

According to the KKT conditions of optimal problems, we can get the threshold value b:

$$b = \begin{cases} y_i - \omega \cdot x_i - \varepsilon, & a_i \in (0, C) \\ y_i - \omega \cdot x_i + \varepsilon, & a_i^* \in (0, C). \end{cases} \tag{4}$$

So the linear regression function is

$$f(x) = \sum_{i=1}^{l} (\alpha_i - \alpha_i^*)(x_i \cdot x) + b. \tag{5}$$

For nonlinear regression problems, the basic idea is that the data is mapped into a high-dimensional feature space via nonlinear mapping, so as to accomplish the linear regression in this space. Its realization is mainly completed through kernel function $K(x, y)$ with the optimization problem as follows:

$$\max \left[-\frac{1}{2} \sum_{i,j=1}^{l} (\alpha_i - \alpha_i^*)(\alpha_j - \alpha_j^*) K(x_i \cdot x_j) + \sum_{i=1}^{l} y_i (\alpha_i - \alpha_i^*) - \varepsilon \sum_{i=1}^{l} (\alpha_i + \alpha_i^*) \right], \tag{6}$$

where $K(x_i \cdot x_j) = \phi(x_i) \cdot \phi(x_j)$ is the kernel function conforming the Mercer conditions.

So the nonlinear regression function can be expressed by

$$f(x) = \sum_{i=1}^{l} (\alpha_i - \alpha_i^*) K(x_i \cdot x) + b, \tag{7}$$

where the sample set in accordance with $(\alpha_i - \alpha_i^*) \neq 0$ is support vector.

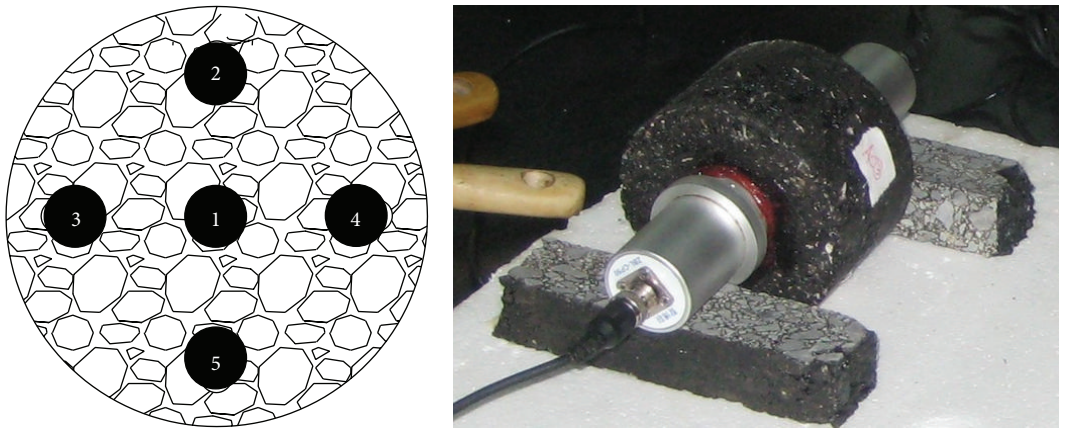

(a) The arrangement of measuring points (b) Ultrasonic detection test

Figure 4: Ultrasonic testing method of asphalt mixture specimen.

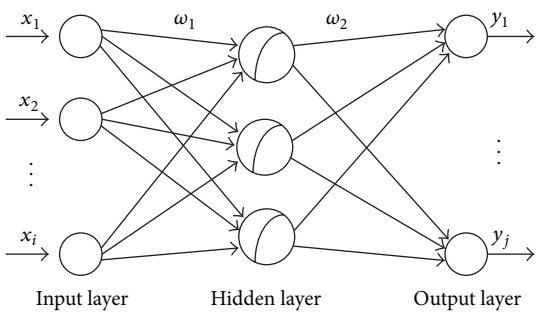

Figure 5: Structure of BP neural network.

2.2.2. BP Neural Network. BP neural network is a multilayer feed forward neural network in one-way transmission. Any non-linear mapping from input to output can be achieved by establishing the relationship between the input and output transfer function [16–18]. The core of BP neural network algorithm is the forward transfer of information and back-propagation of training error. The use of the steepest descent method is adopted to constantly revise each node's weight value and threshold value by error backpropagation [19]. The typical structure of neural network is shown in Figure 5.

2.2.3. Grey Theory. Grey theory is used to solve the problems of analysis, modeling, forecasting, decision making, and control in the grey system [20]. The grey prediction model is an effective tool for dealing with small sample prediction due to its advantages of less modeling information, convenient operation, and high modeling accuracy [21, 22]. In this paper, GM (1, 1) model is used to establish the damage regression model for prediction of asphalt mixture. The modeling process is as follows.

Accumulating the original data sequence $x^{(0)} = [x^{(0)}(1), x^{(0)}(2), \ldots, x^{(0)}(n)]$ to generate 1-AGO sequence $x^{(1)} = [x^{(1)}(1), x^{(1)}(2), \ldots, x^{(1)}(n)]$ and given $z^{(1)}(k) = 0.5x^{(1)}(k) + 0.5x^{(1)}(k-1)$, then the neighbor-generated sequence is

$$z^{(1)} = \left[z^{(1)}(1), z^{(1)}(2), \ldots, z^{(1)}(n)\right]. \tag{8}$$

According to the GM (1, 1) model theory, the grey differential equation is

$$x^{(0)}(k) + az^{(1)}(k) = b, \quad k = 1, 2, \ldots, n, \tag{9}$$

where a is the developed grey number and b is endogenetic control grey number.

If $\widehat{a} = (a, b)^T$ are parameters column, assuming that

$$Y = \begin{bmatrix} x^{(0)}(2) \\ x^{(0)}(3) \\ \vdots \\ x^{(0)}(n) \end{bmatrix}, \qquad B = \begin{bmatrix} -z^{(0)}(2) & 1 \\ -z^{(0)}(3) & 1 \\ \vdots & \vdots \\ -z^{(0)}(n) & 1 \end{bmatrix}, \tag{10}$$

then the least-square-estimation parameters column of the grey differential equation will satisfy

$$\widehat{a} = \left(B^T B\right)^{-1} B^T Y. \tag{11}$$

Taking $x^{(0)}(1) = x^{(1)}(0)$, then the solution of the winterization equation $dx^{(1)}/dt + ax^{(1)} = b$ is

$$x^{(1)}(k+1) = \left[x^{(0)}(1) - \frac{b}{a}\right] e^{-ak} + \frac{b}{a}, \quad k = 1, 2, \ldots, n. \tag{12}$$

Therefore, the restored value is

$$x^{(0)}(k+1) = x^{(1)}(k+1) - x^{(1)}(k), \quad k = 1, 2, \ldots, n. \tag{13}$$

3. Results and Discussions

3.1. W-T-R Cycle Test and Ultrasonic Detection of Asphalt Mixture. The air void (VV) of specimens in different cycles

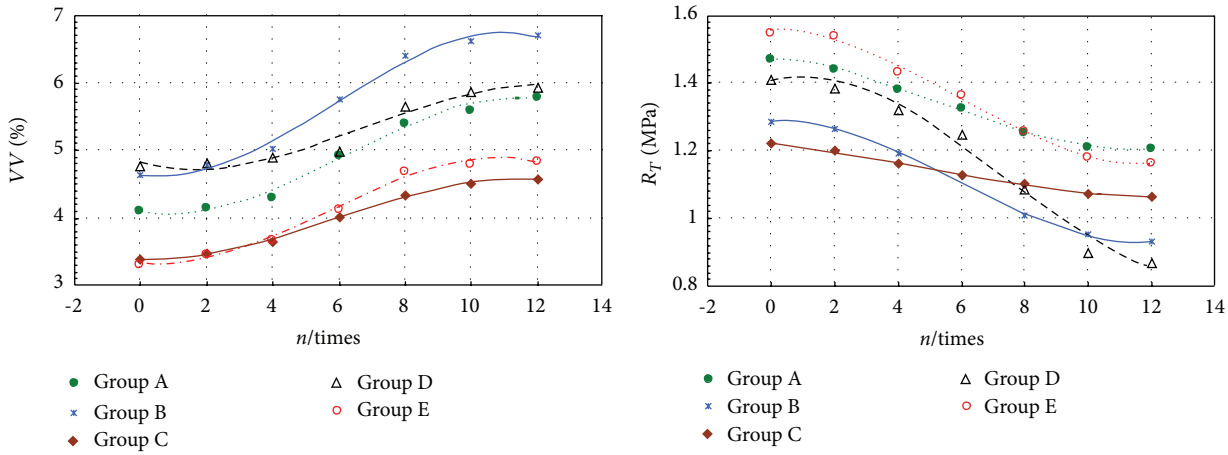

(a) Changes of VV-n (b) Changes of R_T-n

Figure 6: Testing results of VV and R_T.

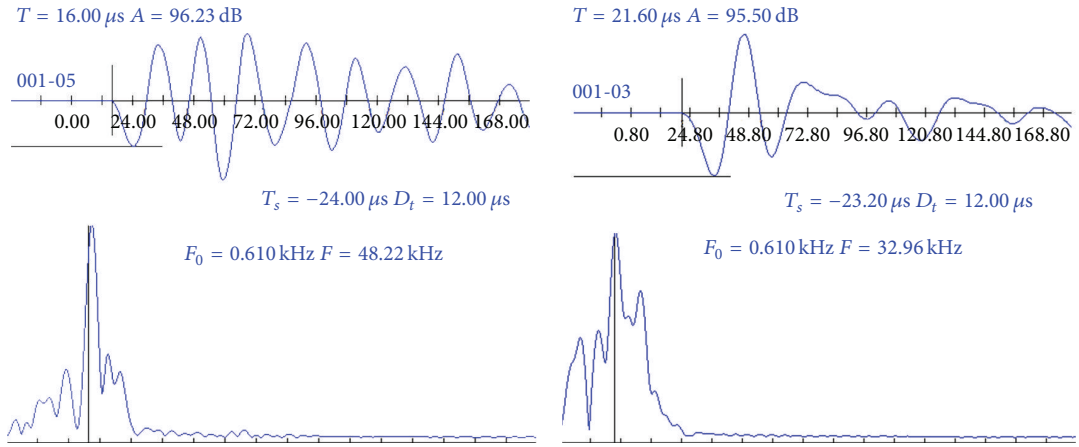

(a) Waveform and spectrum before the damage (b) Waveform and spectrum after the damage of 12 cycles

Figure 7: Waveform and spectrum before and after the damage.

is measured at 20°C using surface-dry method. The indirect tensile tests are conducted with the help of MTS multifunctional test machine in order to obtain the splitting strength (R_T). The results of VV, R_T and the number of cycles (n) are shown in Figure 6.

In the process of W-T-R cycles, five groups of the specimen are subjected to ultrasonic test. The typical waveform and spectrum before and after damage are shown in Figure 7.

From Figure 6, the following can be seen: (1) With the increase of asphalt-aggregate ratio and striking times, the initial void ratio of specimen reduces. The specimen will be more closed as the asphalt-aggregate ratio and striking times increase. (2) The initial strength of test specimen will reduce no matter the asphalt-aggregate ratio increases or reduces. However, the increase of striking times will enhance it. Excessive asphalt on the surface of aggregates will play the role of lubrication, and inadequate asphalt cannot provide a sufficient cohesive force. Thus, both too much and too little asphalt will reduce the initial strength of the test specimen. Besides, the increase of striking times will strengthen the overall stability of the test specimen and improve its initial strength. (3) In the process of water-temperature-radiation cycles, the varied amplitude of void ratio reduces as the asphalt-aggregate ratio and striking times increase. As the asphalt-aggregate ratio and striking times increase, the void ratio will reduce, the integrity will enhance, and the infiltration moving water will reduce. Thus, the interdeformation of specimen will be constrained when the temperature changes. Therefore, the changes of void ratio will be restricted. (4) In the process of water-temperature-radiation cycles, increase of the asphalt-aggregate ratio will slow down the damage of test specimen. However, the damage of test specimen increases as the striking times increase. The higher asphalt content would make the asphalt mastic fully contact with the surface of aggregate and retain the bonding capacity and toughness to effectively resist the hydrodynamic erosion. Thus, the strength of asphalt mixture attenuation is more slowly. If there are too many striking times on the specimen,

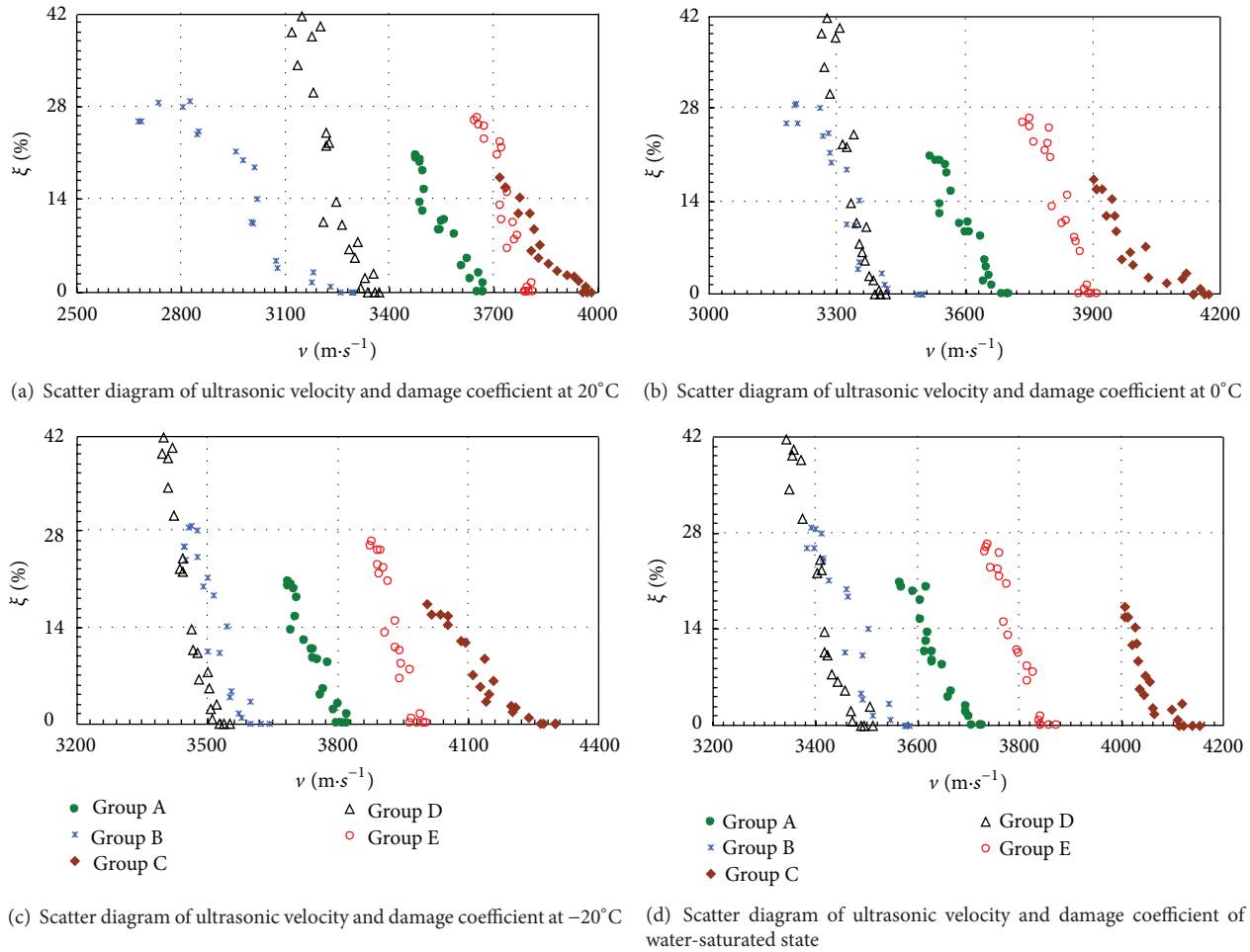

(a) Scatter diagram of ultrasonic velocity and damage coefficient at 20°C

(b) Scatter diagram of ultrasonic velocity and damage coefficient at 0°C

(c) Scatter diagram of ultrasonic velocity and damage coefficient at −20°C

(d) Scatter diagram of ultrasonic velocity and damage coefficient of water-saturated state

FIGURE 8: Scatter diagram of ultrasonic velocity and damage coefficient.

the edge of aggregate will fragment and the aggregates cannot fully interlock with each other. Thus, the strength of specimen will reduce.

From Figure 7, the ultrasonic parameters of test specimen vary after W-T-R cycle tests: (1) *Waveform Distortion*. The waveform after damage appears disorganized, accompanied with multipeak phenomenon and obvious amplitude attenuation. This is due to the increase of specimen porosity after W-T-R cycles. When the ultrasonic wave is propagating in the damaged specimen, the different actions, for example, diffraction, reflection, and refraction will appear in the injury interface. Since the ultrasonic signal is superimposed, the waveform becomes distorted. The more severe the waveform distortion is, the more serious the extent and scope of damage is. (2) *Frequency Reduction*. When ultrasonic wave is propagating in the damaged specimen, the acoustic energy attenuation occurs, and different frequency components have different attenuation degrees. Compared to the lower frequency portion, the attenuation degree of the high-frequency portion is more severe. Thus, the main frequency of the received wave drifts to the low frequency. (3) *Velocity Decrease*. Integrity of the specimen is destructed because of the action of W-T-R cycles. A large number of voids occur in the interior of specimen. Since the acoustic impedance ratio of the air in the voids is much smaller than that of the aggregate and asphalt film, the ultrasonic pulse wave has to spread around the voids. Thus, with the propagation distance increasing, the measured acoustic time increases as well.

The characteristic changes of ultrasonic waveform, spectrum, and velocity can be used to make a preliminary judgment on asphalt mixture damage after the action of W-T-R cycles and construct the prediction models.

3.2. Damage Model of Asphalt Mixture under the Action of W-T-R Cycle. In order to distinguish the influence of different temperatures and water content on the ultrasonic velocity, ultrasonic tests are conducted under the conditions of 20°C, 0°C, −20°C, and water saturated. The saturation process is as follows. Firstly, the specimen is saturated in the vacuum saturation instrument (LCD-2, Hebei Rongda Co., Ltd., China) under 98 KPa for 15 min. Then, the specimen stayed in the water under constant pressure for 0.5 h.

We assume the splitting tensile strength as the damage index, and the damage parameter ξ is defined as follows:

$$\xi_i = \left(1 - \frac{I_i}{I_0}\right) \times 100\%, \tag{14}$$

Table 3: Regression and prediction results of SVM, BP, and grey theory.

Conditions	Groups number	Square error (%)			Prediction error (%)		
		SVM	BP neural network	Grey theory	SVM	BP neural network	Grey theory
20°C	A	0.010	0.029	0.089	1.09	0.92	25.76
	B	0.006	0.021	0.068	5.33	3.45	13.69
	C	0.004	0.019	0.091	8.62	7.19	8.50
	D	0.012	0.048	0.062	2.20	3.20	12.02
	E	0.013	0.043	0.064	2.83	6.28	17.57
0°C	A	0.012	0.038	0.103	9.63	2.92	12.03
	B	0.007	0.028	0.072	4.49	4.99	22.48
	C	0.010	0.018	0.071	0.59	4.46	23.19
	D	0.010	0.027	0.074	5.48	12.22	10.15
	E	0.010	0.033	0.053	0.04	4.44	13.59
−20°C	A	0.010	0.028	0.093	6.63	23.80	9.02
	B	0.012	0.036	0.073	0.69	2.80	8.63
	C	0.006	0.019	0.035	7.91	0	16.05
	D	0.004	0.011	0.093	2.56	4.38	9.69
	E	0.011	0.033	0.073	1.42	15.74	12.37
Water-saturated state	A	0.010	0.039	0.094	9.42	13.99	9.68
	B	0.012	0.045	0.096	5.14	4.49	7.10
	C	0.008	0.030	0.032	5.77	11.77	25.98
	D	0.004	0.011	0.085	4.87	4.15	7.71
	E	0.007	0.016	0.100	5.90	2.26	18.64

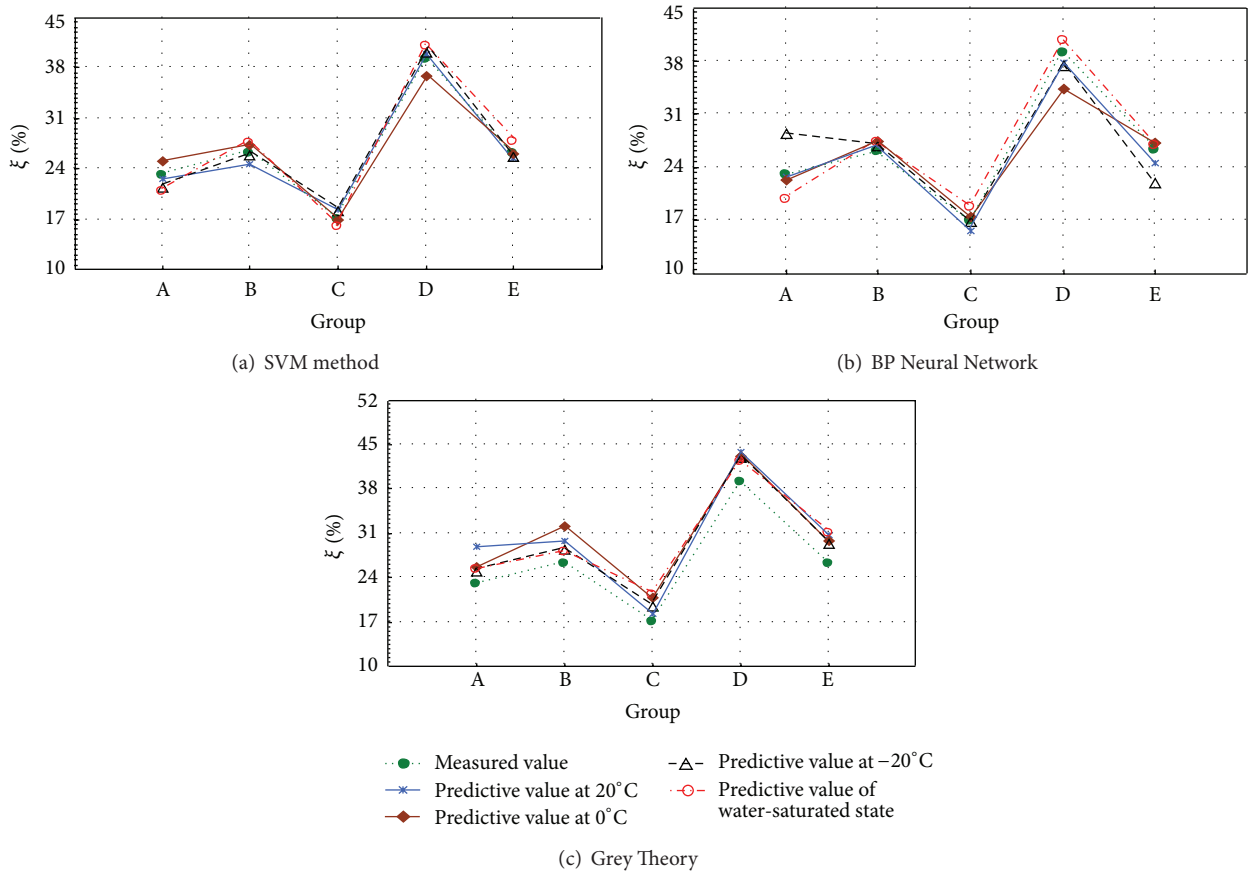

(a) SVM method

(b) BP Neural Network

(c) Grey Theory

Figure 9: Comparison picture between prediction and actual value.

where, I_0 and I_i are the splitting tensile strength without and with W-T-R cycles, respectively, i is the W-T-R cycle times.

The scatter diagrams of the relationship between ultrasonic velocity and damage coefficient under different conditions are shown in Figure 8.

The ultrasonic velocity is selected as independent variable and the damage coefficient as dependent variable. Then, they can be normalized by the following equation:

$$X = (\lambda_{\max} - \lambda_{\min}) \times \frac{(x - x_{\min})}{(x_{\max} - x_{\min})} + \lambda_{\min}, \quad (15)$$

where x is the original data; X is the normalized data; $\lambda_{\max}$ and $\lambda_{\min}$ are the mapped range parameters. In this paper, $\lambda_{\max} = 1$, $\lambda_{\min} = -1$.

Twelve groups of testing data under W-T-R cycles are treated as training samples, and the radial basis function is selected as kernel function. K-ford cross validation (K-CV) algorithm is used for cross-validation of original data. The optimal values of penalty factor C and kernel-function parameter g are determined by controlling the mean square error. The calculated optimum parameters are used to train SVM for establishing the regression model of predicting.

Neural network includes three layers. The input vectors are the times of W-T-R cycles and ultrasonic velocity, while the output vector is damage coefficient. Therefore, the number of input-layer node is 2 and output-layer node number is 1. The hidden-layer node number should be determined through trial-and-error method. After several-time tests, it is fixed on 5 in the final. Momentum BP algorithm is used to train the sample data until the learning error below 0.001 or the training times higher than 10000 times.

The original data will be equal-interval treated by Lagrange's interpolation. For filtering the random fluctuation of the data, moving average method is introduced to treat the original sequence. And then, the gray GM (1, 1) model is built.

Another two samples of W-T-R cycle tests are used for validating and comparing the performance of three models derived from SVM, neural network, and grey theory. The mean square error of fitting and predication are listed in Table 3, and measured values are compare with predictive values in Figure 9.

From the fitting and prediction performance of each of the three models, it can be concluded as follows.

(1) The fitting results by SVM method are better than BP neural network and grey theory. The maximum mean square error by SVM, BP neural network, and grey theory is 0.013, 0.048, and 0.103, respectively, while the minimum mean square error by the three methods is 0.004, 0.011, and 0.032, respectively. Besides, SVM method is able to overcome the problem of aimless trial calculation by selecting different penalty factor C and kernel-function parameter g by the method of cross-validation. *Thus,* the operation efficiency is largely improved. In conclusion, SVM method can consider all data and has lower jumping process and higher fitting precision. It is able to avoid over fitting or under fitting, and effectively reflects the relationship between ultrasonic velocity and damage coefficient.

(2) Comparing with actual data, the forecasting precision of SVM is also higher than BP neural network and grey theory. The maximum forecasting relative error of SVM is 9.63%, but the minimum forecasting relative error is 0.04%. For BP neural network, the largest forecasting relative error is 23.8% but the smallest is 0. For grey method, the maximum forecasting relative error is 25.98% while the minimum is 7.10%, the forecasting precision of which is obviously lower than the first two methods. From this, we can conclude that SVM method has higher precision and better stability. It is an ideal method for solving non-linear problems of simple sample, and has stronger generalization ability.

4. Conclusions

Based on the results of experimental work and the discussion in this study, the following conclusions can be drawn.

(1) W-T-R cycle simulation system can accurately simulate the environmental effects of heavy rain, high temperatures and intense radiation, which can comprehensively reflect the asphalt mixture damage in practice.

(2) With the increase of asphalt amount and striking times, the initial void ratio and varied amplitude reduce. The initial strength of test specimen will reduce no matter the asphalt-aggregate ratio increases or reduces. However, the increase of striking times will enhance it. Increase of the asphalt-aggregate ratio will slow down the damage of test specimen.

(3) Ultrasonic detection method can quickly evaluate the damage state of asphalt mixture after the action of W-T-R cycles and effectively predict the damage degree. Firstly, the characteristic changes of ultrasonic waveform, spectrum, and velocity can be used to make a preliminary judgment on asphalt mixture damage after the action of W-T-R cycles. Then, the regression models for prediction between ultrasonic velocity and damage coefficient are established for specifically evaluating the damage degree of the specimen.

(4) SVM regression prediction method possesses more favorable accuracy and stability as well as strong generalization ability, and it can accurately reflect the relationship between ultrasonic velocity and damage coefficient. Therefore, this method can rapidly evaluate the damage state of asphalt mixture with strong practical significance.

Acknowledgment

The authors gratefully acknowledge the support of the National Natural Science Foundation of China (Project nos. 51278222 and 51378236).

References

[1] E. Iskender and A. Aksoy, "Field and laboratory performance comparison for asphalt mixtures with different moisture conditioning systems," *Construction and Building Materials*, vol. 27, no. 1, pp. 45–53, 2012.

[2] H. Fazaeli, H. Behbahani, A. A. Amini, J. Rahmani, and G. Yadollahi, "High and low temperature properties of FT-paraffin-modified bitumen," *Advances in Materials Science and Engineering*, vol. 2012, Article ID 406791, 7 pages, 2012.

[3] Y.-Q. Tan, X.-L. Li, and B. Hu, "Influence of dynamic water on the anti-cracking performance of asphalt mixture at low temperature," *Journal of Harbin Institute of Technology*, vol. 42, no. 1, pp. 119–122, 2010.

[4] L. Li and S. Tong, "Laboratory evaluation of ultraviolet radiation for asphalt pavement performance in desert regions," *Materials Science Forum*, vol. 695, pp. 481–484, 2011.

[5] W.-H. Jiang, X.-N. Zhang, and Z. Li, "Mechanical mechanism of moisture-induced damage of asphalt mixture based on simulation test of dynamic water pressure," *China Journal of Highway and Transport*, vol. 24, no. 4, pp. 21–25, 2011.

[6] H. S. Shang and T. H. Yi, "Behavior of HPC with fly ash after elevated temperature," *Advances in Materials Science and Engineering*, vol. 2013, Article ID 478421, 7 pages, 2013.

[7] M. Tigdemir, S. F. Kalyoncuoglu, and U. Y. Kalyoncuoglu, "Application of ultrasonic method in asphalt concrete testing for fatigue life estimation," *NDT and E International*, vol. 37, no. 8, pp. 597–602, 2004.

[8] J. Y. Yi, D. C. Feng, G. W. Wang, and Z. S. Yu, "Application of ultrasonic test method in freeze-thaw test of asphalt mixture," *Journal of Highway and Transportation Research and Development*, vol. 26, no. 11, pp. 6–10, 2009.

[9] H. Zheng and H. Lu, "A least-squares support vector machine (LS-SVM) based on fractal analysis and CIELab parameters for the detection of browning degree on mango (Mangifera indica L.)," *Computers and Electronics in Agriculture*, vol. 83, pp. 47–51, 2012.

[10] V. N. Vapnik, *The Nature of Statistical Learning Theory*, Springer, New York, NY, USA, 1995.

[11] M. Fauvel, J. Chanussot, J. A. Benediktsson, and A. Villa, "Parsimonious Mahalanobis kernel for the classification of high dimensional data," *Pattern Recognition*, vol. 46, no. 3, pp. 845–854, 2013.

[12] A. Chamkalani, A. H. Mohammadi, A. Eslamimanesh, and F. Gharagheizi, "Diagnosis of asphaltene stability in crude oil through "two parameters" SVM model," *Chemical Engineering Science*, vol. 81, pp. 202–208, 2012.

[13] P. Du, K. Tan, and X. Xing, "Wavelet SVM in Reproducing Kernel Hilbert Space for hyperspectral remote sensing image classification," *Optics Communications*, vol. 283, no. 24, pp. 4978–4984, 2010.

[14] S. Pang, T. Ban, Y. Kadobayashi, and N. Kasabov, "Personalized mode transductive spanning SVM classification tree," *Information Sciences*, vol. 181, no. 11, pp. 2071–2085, 2011.

[15] S. Ch, N. Anand, B. K. Panigrahi, and S. Mathur, "Stream flow forecasting by SVM with quantum behaved particle swarm optimization," *Neurocomputing*, vol. 101, pp. 18–23, 2013.

[16] Y. T. Hong, "Dynamic nonlinear state-space model with a neural network via improved sequential learning algorithm for an online real-time hydrological modeling," *Journal of Hydrology*, vol. 468-469, pp. 11–21, 2012.

[17] T. S. Ozsahin and S. Oruc, "Neural network model for resilient modulus of emulsified asphalt mixtures," *Construction and Building Materials*, vol. 22, no. 7, pp. 1436–1445, 2008.

[18] P. H. S. W. Kulatilake, W. Qiong, T. Hudaverdi, and C. Kuzu, "Mean particle size prediction in rock blast fragmentation using neural networks," *Engineering Geology*, vol. 114, no. 3-4, pp. 298–311, 2010.

[19] K. Golzar, A. J. Arani, and M. Nematollahi, "Statistical investigation on physical-mechanical properties of base and polymer modified bitumen using artificial neural network," *Construction and Building Materials*, vol. 37, pp. 822–831, 2012.

[20] L.-H. Jiang, A.-G. Wang, N.-Y. Tian, W.-C. Zhang, and Q.-L. Fan, "BP neural network of continuous casting technological parameters and secondary dendrite arm spacing of spring steel," *Journal of Iron and Steel Research International*, vol. 18, no. 8, pp. 25–29, 2011.

[21] M. S. Yin, "Fifteen years of grey system theory research: a historical review and bibliometric analysis," *Expert Systems with Applications*, vol. 40, no. 7, pp. 2767–2775, 2013.

[22] J. Wei and Y. Zhang, "The application of Grey system theory to correlate chemical composition and surface free energy of asphalt binders," *Petroleum Science and Technology*, vol. 28, no. 17, pp. 1807–1817, 2010.